

## **APPLICATION OF WAVELET TRANSFORM IN TARGET IDENTIFICATION**

*H. J. Li and K. M. Li*

- 1. Introduction**
  - 2. Wavelet Transform and Multiscale Edge Detection**
  - 3. Application of Wavelet Transform to Feature Representation**
  - 4. Recognition Performance**
  - 5. Discussion and Conclusion**
- Acknowledgment**  
**References**

### **1. Introduction**

Numerous research studies on target identification have been proposed in the past several years [1–7]. All methods have to deal with scattered fields which are highly dependent on frequency, polarization, and target aspect. To reduce the complex dependence the scattered fields are usually converted into the time-domain, including the late-time response which includes the natural frequencies of the target [2,6] and the early time response (or the range profile) which provides detailed information about the target [4,5]. A remarkable advantage of the late-time response is its aspect independence which eliminates the need for storage of aspect-dependent information [2]. However, the bandwidth restriction and the lack of directivity of antennas at the low frequencies at which late-time information is available preclude the use of this information.

In contrast, using range profiles as the feature vector representation for aerospace target identification has been proved simple, robust, and range-insensitive [4,5]. However, range profiles are aspect-

dependent. Requirements for aspect increment in order to obtain a useful but not wasteful data storage have been discussed in [8]. It was found that a radar with higher range resolution can tolerate more aspect variation, yielding a significant advantage in saving memory space for establishing the data base, yet it requires a higher sampling of data for each range profile. A one-dimensional discrete wavelet transform on the early-time response has been proposed to reduce the amount of data that must be stored for each aspect angle [7]. In this paper we will also apply the wavelet transform to reduce the data storage space, but treat it from a different point of view.

The wavelet transform was originally developed to overcome the inherent fixed resolution property of the short-time Fourier transform. The wavelet transform uses multiscale windows and is more efficient at providing multiscale resolution [9,10]. The wavelet transform is also closely related to multiscale edge detection [11]. This property will be used to compress the data base and to identify a target.

The paper is organized as follows. A brief review of the wavelet transform theory and multi-scale edge detection is presented in Section II. The method of applying the wavelet transform to radar signal processing and the procedure of establishing the compressed data base will be described in Section III. In Section IV the decision rules and the effect of Gaussian noise on the recognition performance will be discussed. The recognition performance obtained by different data bases and discrimination schemes will be compared as well. Finally, a few concluding remarks summarize the paper.

## 2. Wavelet Transform and Multiscale Edge Detection

The relation between wavelet transform and multiscale edge detection was first discussed by Mallat and Zhong [11]. An introduction to wavelet theory can be found in [10,13]. Let  $h_s(x)$  be the dilation of any function  $h(x)$  by scaling factor  $s$ , i.e.,

$$h_s(x) = (1/s)h(x/s) \quad (1)$$

A wavelet transform is computed by convolving the signal with a dilated wavelet. The wavelet transform of  $f(x)$  at the scale  $s$  and position  $x$ , computed with respect to the wavelet  $\varphi(x)$ , is defined by

$$WF(s, x) = f * \varphi_s(x) \quad (2)$$

where ‘ $*$ ’ denotes convolution. From this equation we know that the wavelet transform can be thought as a kind of bandpass filter operation; its bandwidth can be adjusted by changing the scaling factors [12].

Most multiscale edge detectors smooth the signal at various scales and detect sharp variation points from their first-order derivative. So, if we suppose that  $\varphi(x)$  is the first-order derivative of a smoothing function  $\theta(x)$ , ( $\theta(x)$  converges to 0 at infinity and its integral is equal to 1), i.e.,

$$\varphi(x) = d\theta(x)/dx \quad (3)$$

We can show that

$$WF(s, x) = f*(s d\theta_s/dx)(x) = s \frac{d}{dx}(f*\theta_s)(x) \quad (4)$$

The wavelet transforms  $WF(s, x)$  are the first derivative of the signal smoothed at the scale  $s$ . The local extrema of  $WF(s, x)$  thus correspond to the inflection points of  $f*\theta_s(x)$  and the extrema detection corresponds to an edge detection [11]. The maxima of the absolute value of the first derivative are sharp variation points of  $f*\theta_s(x)$ , whereas the minima correspond to slow variations. We can easily select the sharp variation points by detecting only the local maximum of  $|WF(s, x)|$ . When the scale  $s$  is large, the convolution with  $\theta_s(x)$  removes small signal fluctuations. We therefore only detect the sharp variations of large structures. Besides detecting local maxima, we can also record values of  $WF(s, x)$  at the maximum locations, which measure the derivatives at the inflection points.

### 3. Application of Wavelet Transform to Feature Representation

As indicated in the previous section the wavelet transform is related to multiscale edge detection and the local maximum of  $|WF(s, x)|$  corresponds to the sharp variation points. It is known that positions of sharp variation are the most important feature of a 1-D curve. In this section we will describe how to apply wavelet transform in feature representation.

Five airplane models are chosen as known targets. They are: a C-130 model, an AH-64 helicopter model, a B-52 bomber model, a

SR-71 spy plane model and a space shuttle model. Their physical sizes range from 40 cm to 80 cm and within 12 cm in height. Zero degrees in the azimuthal direction is defined as in the head-on direction and  $90^\circ$  is the fuselage direction. For each object three independent experiments are conducted at three elevation angles,  $\theta = 0^\circ$ ,  $10^\circ$ , and  $20^\circ$ . For each elevation angle the object is rotated from  $\varphi = -6^\circ$  to  $24^\circ$  with an increment of  $0.6^\circ$  and there are 51 total aspects observed. For each aspect the fields with range corrected with respect to the rotational center are measured at step frequencies ranging from 6 GHz to 16 GHz with an increment of 0.1 GHz. The range profile of each aspect is obtained by Fourier transforming the field with respect to  $2k = 4\pi f/c$ , where  $f$  is the frequency and  $c$  is the speed of light. We choose the absolute value of the range profile and the feature vector rather than the complex form or the real part of the range profile. The reason for choosing the absolute value form is the much higher tolerance of angular estimation error or frequency discrepancy, especially in the case of a real target of size as large as 30m [8]. It was found that the complex form can not tolerate an aspect variation as small as  $0.03^\circ$  while the absolute value form can tolerate as great as  $3^\circ$  variation [8]. Range profile of each aspect is represented by 64 sampling points. It has been suggested that direct correlation of target range profiles with their stored counterparts provides a simple, robust, and range-shift-insensitive method for target identification [4,5]. However, storing complete range profiles at many aspects for each target requires massive memory space. In the following we will combine the wavelet transform and the local maximum detection technique to preprocess the range profile and compress the data representation.

The chosen wavelet function and its corresponding smoothing function are shown in Figure 1. This is a quadratic spline of compact support, which has been further defined in [11]. We use the fast wavelet transform algorithm developed by Mallat and Zhong [11] to perform the wavelet transform. This algorithm requires  $O(N \cdot \log_2 N)$  operations for an  $N$ -point data. Shown in Figure 2 are the normalized range profiles of the five targets measured at  $\theta = 10^\circ$  and  $\varphi = 0^\circ$  and their wavelet transforms computed on six scales. We can see that all wavelet transforms look similar when the scale is large. Therefore only the wavelet transforms at  $s = 2^1$ ,  $2^2$ , and  $2^3$  are chosen to represent the target range profiles. As stated in the previous section, a wavelet transform can be thought of as a bandpass filter operation.

Therefore, the three wavelet transforms correspond to the outputs of the range profiles passing through three bandpass filters having the highest frequency passbands. It is noted that the range profiles in the absolute value form are all nonnegative, but their wavelet transform counterparts can be positive or negative as seen in the figures. This is a good property for target discrimination when correlative processing is performed, because the relative distance of the correlation coefficient between correct and wrong targets can be greater as will be seen in the later section.

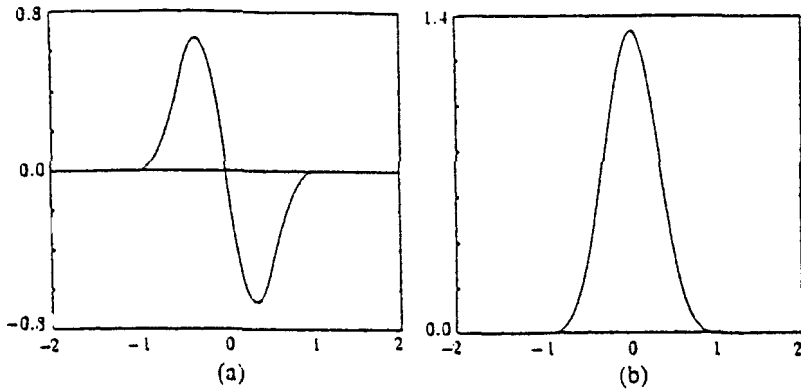


**Figure 1. (a) The chosen wavelet function. (b) The corresponding smoothing function.**

To store the feature representation the wavelet transforms must be discretized. Instead of storing all uniform sampling points we can only store information about local extrema of the  $|WF(m, n)|$  where  $s = 2^m$  and  $m = 1$  or  $2$  or  $3$ . The steps are as follows: For each scale  $2^m$ , find all points  $n$  such that  $|WF(m, n)|$  is greater than  $|WF(m, n-1)|$  and  $|WF(m, n+1)|$ . After that, record these extrema points' locations and their values  $WF(m, n)$ . As stated in Section II, this operation is equivalent to multiscale edge detection. After edge detection, the wavelet transforms shown in Figure 2(a) become as those shown in Figure 3. It is easily observed that the number of peak points has been reduced and most points have very small values close to zero. Therefore we can set a threshold value and store only those points exceeding the threshold and discard all others, yielding a reduction in data storage.

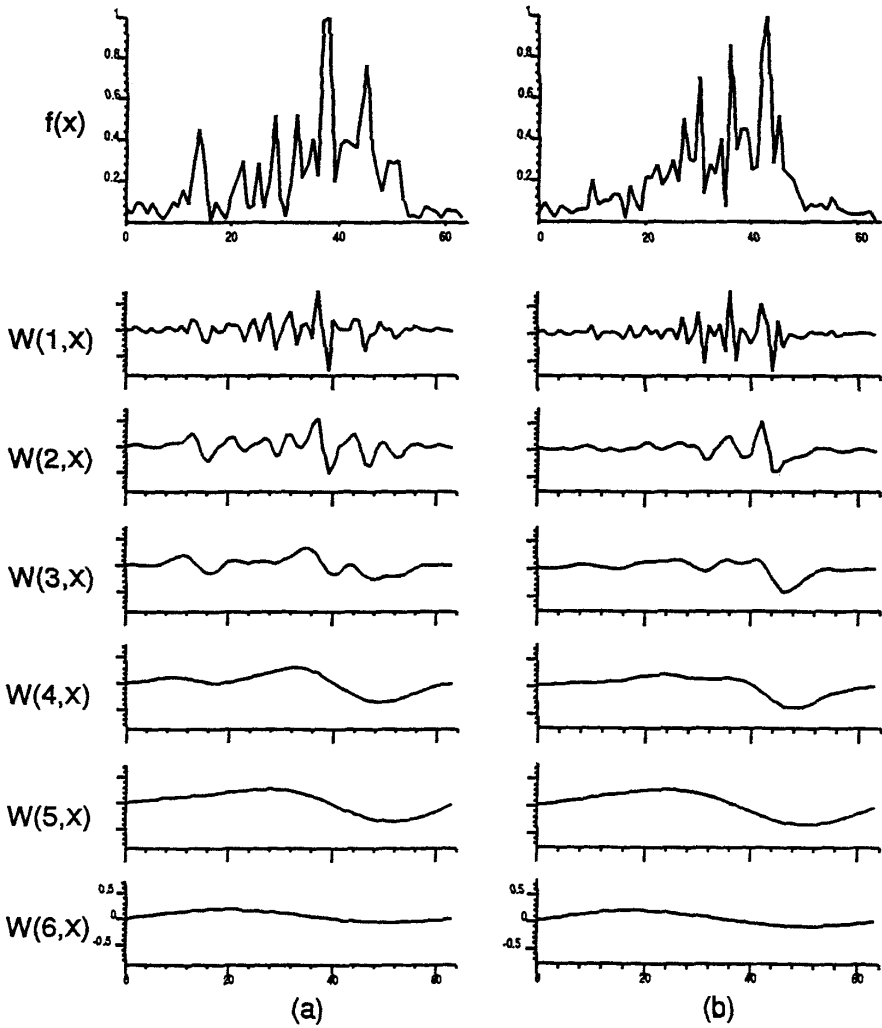


Figure 2. Range profiles and their wavelet transforms computed in six scales, the targets, (a) AH-64, (b) B-52.

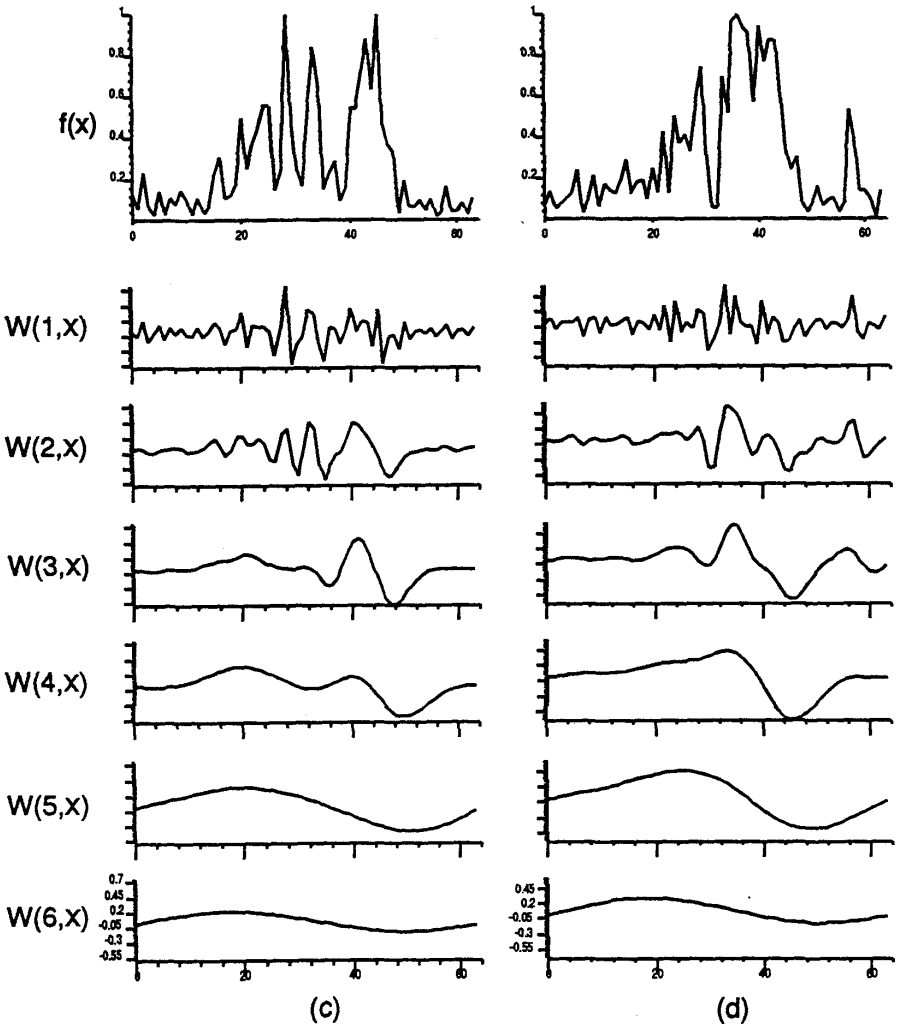


Figure 2. Range profiles and their wavelet transforms computed in six scales, the targets, (c) SR-71, (d) C-130.

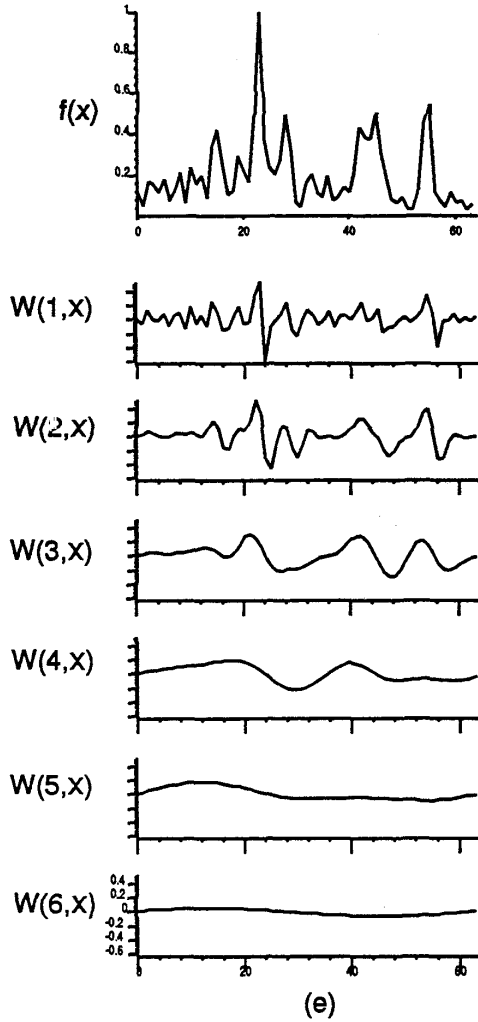


Figure 2. Range profiles and their wavelet transforms computed in six scales, the targets, (e) Space shuttle.

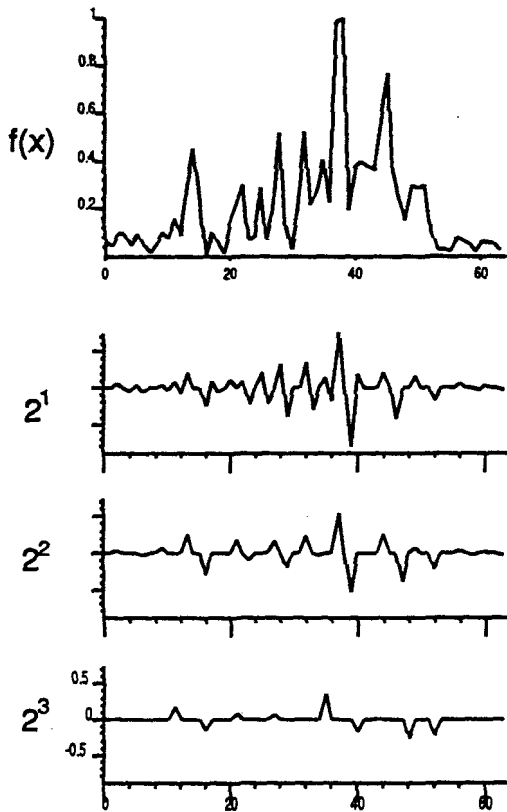


Figure 3. Results after multiscale edge detection.

All range profiles measured at  $\theta = 10^\circ$  are wavelet transformed, edge detected, and stored as the data base. The data sets corresponding to  $s = 2^1$ ,  $2^2$ , and  $2^3$  are denoted by DATA-1, DATA-2, and DATA-3 respectively. After edge detection different range profiles have different number of peaks. The average number of peaks averaged for all five targets and 51 aspects for the three scales  $2^1$ ,  $2^2$ , and  $2^3$  are 42, 21, and 11 respectively and are shown in the first three rows of Table 1. It is seen the average number of peak points for the scale  $2^1$  is 42, which is not much smaller than 64, the original number of points stored for a range profile. If we set the threshold values as 10%, 20%, and 30% of the largest value respectively, their average number of peaks are reduced

to 24, 25, and 9 and are shown in the last three rows of Table 1. The corresponding data sets are denoted by DATA-4, DATA-5, and DATA-6. Clearly, the amount of data to be stored has been compressed. The compression ratio seems not as great as reported in [7], where a range profile is represented by 256 points and the 32 largest wavelet coefficients are stored, yielding a compression ratio of 8. However, the average number of peaks to be stored for DATA-4 is 24, which is smaller than 32.

<i>Data name</i>	<i>Scale</i>	<i>Threshold</i>	<i>number of stored points</i>	<i>compression ratio</i>
<b>Data 1</b>	$2^1$	0	<b>42</b>	<b>1.01</b>
<b>Data 2</b>	$2^2$	0	<b>21</b>	<b>2.03</b>
<b>Data 3</b>	$2^3$	0	<b>11</b>	<b>3.88</b>
<b>Data 4</b>	$2^1$	0.05	<b>24</b>	<b>1.78</b>
<b>Data 5</b>	$2^1$	0.1	<b>15</b>	<b>2.84</b>
<b>Data 6</b>	$2^1$	0.15	<b>9</b>	<b>4.74</b>

Table 1. Number of stored points and compression ratio for different data sets.

Next we calculate the data compression ratio obtained by the proposed method and the range profile method. The proposed method requires 4 bytes and 2 bytes to store a floating point and an integer point respectively. An uncompressed range profile has 64 floating sampling points and needs  $64 \times 4$  bytes, while the compressed one needs 2 bytes to store the location and 4 bytes to store the amplitude for each peak point. Therefore the compression ratio can be calculated by

$$\frac{64 \times 4}{\text{no. of maxima} \times (4 + 2)} = \frac{64}{\text{no. of maxima} \times 1.5}$$

Results of compression ratio for different scales and different thresholds are shown in Table 1.

#### 4. Recognition Performance

In this section we compare recognition performances obtained by different feature vector representations. The decision rule to be used in target identification is the matching score method [4,5], which is summarized as follows:

Given two real feature vectors  $f_1(x)$  and  $f_2(x)$ , the normalized correlation coefficient at a range shift  $\Delta x$  is defined by

$$C_{12}(\Delta x) = \frac{\left| \int f_1(x) f_2(x + \Delta x) dx \right|}{\left| \int |f_1(x)|^2 dx \cdot \int |f_2(x)|^2 dx \right|^{1/2}}$$

Schwartz's inequality states that  $0 \leq C_{12}(\Delta x) \leq 1$ . Assume  $C_{12}(\Delta x_0)$  is the maximum of  $C_{12}(\Delta x)$  for all range shifts, then  $C_{12}(\Delta x_0)$  is called the matching score for the two feature vectors  $f_1$  and  $f_2$  and is denoted by  $C(f_1, f_2)$ .

Let the data base consist of feature vectors  $\{g_{ij}(x)\}$ , where  $g_{ij}(x)$  is the  $j$ th vector in the predefined class. For an incoming feature vector  $f(x)$  belonging to an unknown class, the decision rule is:

Calculate the matching scores,  $C(f, g_{ij})$ , for all possible  $g_{ij}(x)$ . Determine  $f(x)$  to be in class  $i_0$  if  $C(f, g_{i_0 j_0}) \geq C(f, g_{ij})$  for any class-feature pair  $(i, j)$  other than  $(i_0, j_0)$ .

For an incoming target, the measured quantity is the range profile. We then wavelet transform the measured range profile and find its local maxima, and then use the results as the feature vector  $f(x)$ . The matching scores are then calculated by correlating  $f(x)$  with all  $\{g_{ij}(x)\}$  stored in the data base. One may also convert each stored  $g_{ij}(x)$  into a range profile waveform  $g'_{ij}(x)$  through an inverse wavelet transform, and then calculate matching scores between the measure range profile and the converted range profiles  $\{g'_{ij}(x)\}$  as was done in [7]. The latter method requires inversely wavelet transforming all feature vectors stored in the data base, while the former only requires one wavelet transform and can save much computing time.

There are also two methods to calculate the matching scores. One is to calculate the correlation coefficients of  $f(x)$  and  $g_{ij}(x)$  at every  $\Delta x$  and then to choose the largest one. This can be obtained by using the efficient inverse FFT method. The order of the operations is  $(3N \log_2 N)$  for an  $N$ -point feature vector pair. The second method is to use the centroid-alignment method [5], which is to preprocess all range profiles by finding their centroids first and then range-shifting them with respect to the centroid. There the feature vectors are all aligned with respect to their centroids. The matching score is then obtained by calculating the correlation coefficient of  $f(x)$  and  $g_{ij}(x)$  with zero range shift. Order of the operation is  $N$ , which is much smaller than  $3N \cdot \log_2 N$ . For a correct recognition, the testing and the stored feature vectors are aligned and will give a maximum correlation coefficient with zero shift. For a wrong pairing, the correlation coefficient so obtained may not be the maximum, but it is desired that the matching score be as small as possible in such a wrong pairing case. In the following we use the centroid-alignment method to identify targets.

In a real radar system, noise will contaminate the measured range profile and the unknown target aspect may not be at the same condition as it was in establishing the data base. In the following we will examine the effect of Gaussian noise and aspect variation on the recognition performance.

First we define the signal to noise ratio of a complex range profile in the presence of Gaussian noise. Let  $f(x_i)$  represent the  $i$ th sampled value of the complex range profile. The total power of the range profile is defined as  $\sum_{i=1}^N |f^2(x_i)|$ , where  $N$  is the number of sampled points. The Gaussian noise has a variance  $\sigma^2$ . The signal to noise ratio is then defined by  $S_n = \frac{\sum |f(x_i)|^2}{N\sigma^2}$ . In the simulation each sampled value  $f(x_i)$  is added by a complex value  $n_i$ , whose real part and imaginary part are normally distributed with a zero mean and a variance given by  $\sigma^2 = (\sum |f(x_i)|^2)/NS_n$  for a given signal to noise ratio  $S_n$ .

All range profiles measured at elevation angle  $\theta = 10^\circ$  are artificially contaminated with Gaussian noise and are to be identified. For each given  $S_n$ , fifty independent noise sets are added to each range profile. The recognition rate is defined as the percentage of successful identification for all trials ( $50 \times 51 \times 5$  for the present case). Shown in Figure 4 are the average recognition rates by using DATA-1 through DATA-6 and the uncompressed data set (i.e., using the range profile

data directly) for different signal to noise ratios. It is seen all average recognition rates are greater than 60% when the signal to noise ratio is as low as 3 dB. The performance obtained by DATA-5 ( $2^1$  scale and 20% threshold) is better than that obtained by DATA-2 ( $2^2$  scale) although the former has a greater compression ratio. The reason is that wavelet transform with a higher scale will smooth the original curve and lose the subtle distinction. The whole average recognition rate is better than that obtained by the neural network approach (the rates are 72% for  $S_n = 10$  dB and 42% for  $S_n = 5$  dB) [5,14], but is a little worse than that obtained by the uncompressed data set (i.e., using the range profile data directly). Another measure of the quality of the discrimination decision is given by the ratio between the peak correlation and the next largest value [4,7,14]. The greater the ratio, the better the discrimination. Shown in Figure 5 are the ratios for different noise levels. It is seen the ratio obtained by the uncompressed data is the smallest, because elements of such feature vectors are all nonnegative, while the compressed ones have both positive and negative elements as mentioned in Section III.

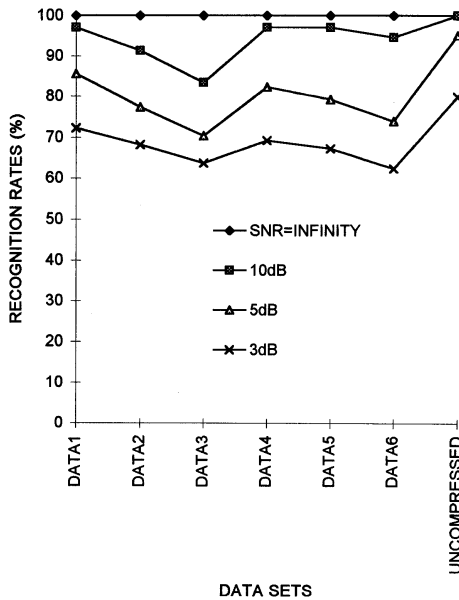


Figure 4. Averaged recognition rates using different data sets with several signal to noise ratios.

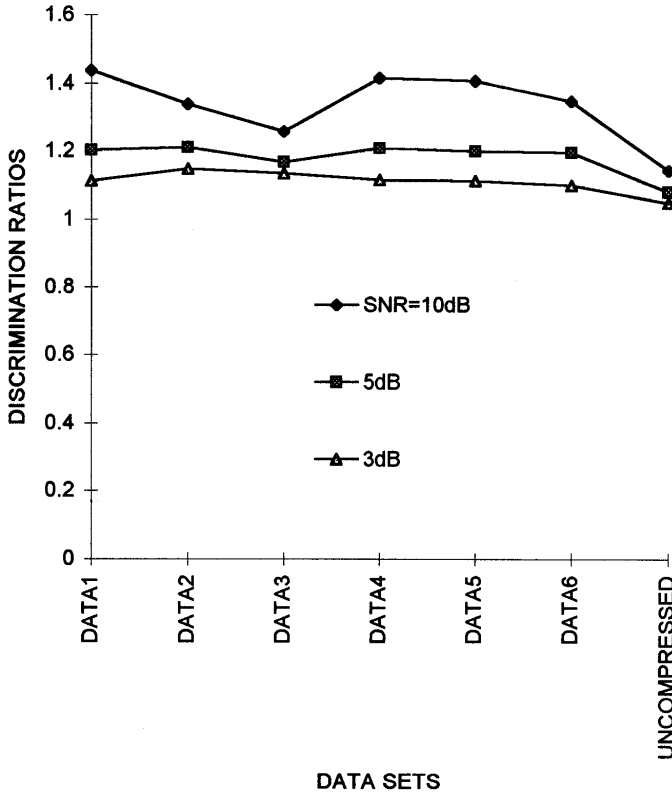


Figure 5. Averaged discrimination ratios using different data sets with several signal to noise ratios.

The immunity to noise contamination shown in Figures 4 and 5 is not as great as that reported in [7]. The range profile used in this paper is in the absolute value form, obtained after incoherent detection, not in the real value form as in [7]. It is known that operations like Fourier transform, wavelet transform, or correlation, are all coherent processes, and can strongly withstand Gaussian noise contamination, especially when the number of data points is very large. But using real or complex range profiles as feature vectors has a big disadvantage, which has been explained in Section III.

Next we use the range profile measured at  $\theta = 0^\circ$  and  $\theta = 20^\circ$  as the testing range profile and compare them with DATA-1 to DATA-6, which are derived from those measured at  $\theta = 10^\circ$ . The recognition rates for each target and the average rate using different data sets are shown in Figure 6. Some targets (space shuttle, C-130 and B-52) have high recognition rates, which means that these targets can tolerate more aspect variation. The SR-71 and AH-64 have very low recognition rates, which implies a  $10^\circ$  variation in elevation is not permissible for faithful recognition. Performance obtained by the uncompressed data is better than those obtained by the compression sets by 5-10%.

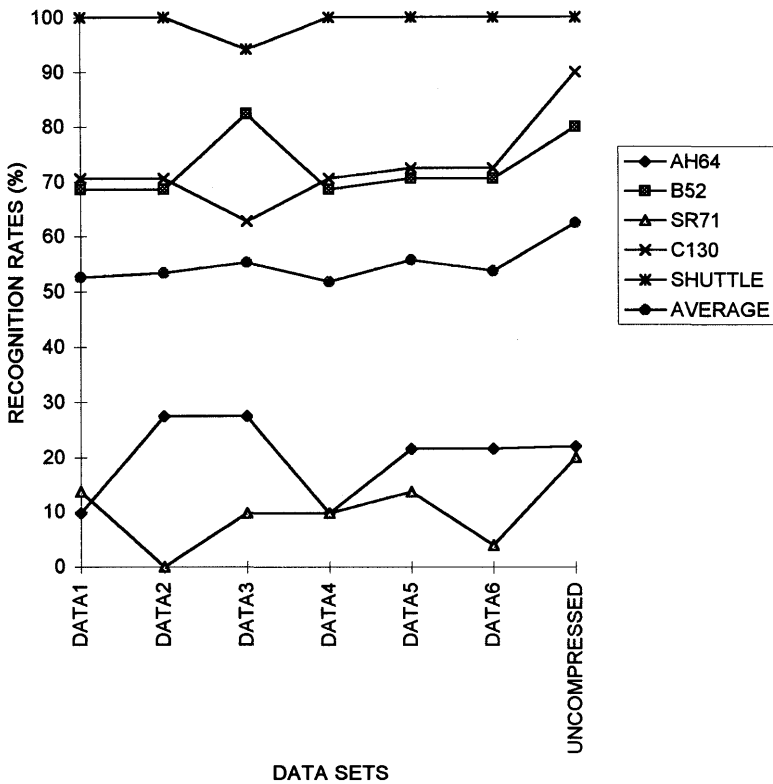


Figure 6. Recognition rates of several targets using different data sets. The unknown feature vectors are measured at  $\theta = 0^\circ, 20^\circ$ , while those stored in the data base are measured at  $\theta = 10^\circ$ .

## 5. Discussion and Conclusion

In this paper we have reviewed the relation between the wavelet transform and the multiscale edge detection and described how to apply the wavelet transform in feature vector representation. To establish the data base the range profile in the absolute value form is first wavelet transformed, and then its local maxima are detected. Only those extrema points exceeding a certain threshold value are stored to represent the feature vector, yielding a reduction in memory storage. When an incoming unknown target is present, the measured range profile is also converted to the same feature vector form. The matching scores are then calculated by correlating the testing feature vector with all those stored in the data base. By range-shifting the measured range profiles with respect to their centroid, the matching scores can be efficiently computed. We have compared the recognition performance when feature vectors are represented with different data compression ratios. When range profiles are contaminated by Gaussian noise, it was found that the recognition rates obtained by the compressed data sets are a little worse than those obtained by the uncompressed data set, but better than those obtained by the neural network approach. The balance between the sacrifice of recognition ratios or the gain of data compression should be justified by the system designer.

## Acknowledgment

This work was supported by the National Science Council, Republic of China, under the contract NSC 84-2213-E-002-054.

## References

1. Moffatt, D. L., J. D. Young, A. A. Ksienski, H. C. Lin, and C. M. Rhoads, "Transient response characteristics in identification and imaging," *IEEE Trans. Antennas and Propagation*, Vol. 29, No. 2, 192–201, 1981.
2. Chen, K. M., D. P. Nyquist, E. J. Rothwell, L. L. Webb, and B. Drachman, "Radar target discrimination by convolution of radar returns with extinction-pulse and single-mode extraction signals," *IEEE Trans. on Antennas and Propagation*, Vol. 34, No. 7, 896–904, 1986.

3. Lin, M. C., Y. W. Kiang, and H. J. Li, "Experimental dimension of wire stick targets using multiple frequency amplitude returns," *IEEE Trans. on Antennas and Propagation*, Vol. 40, No. 9, 1036–1040, 1992.
4. Li, H. J., and S. H. Yang, "Using range profiles as feature vectors to identify aerospace objects," *IEEE Trans. on Antennas and Propagation*, Vol. 41, No. 3, 261–268, 1993.
5. Li, H. J., and V. Chiou, "Aerospace target identification—comparison between the matching score approach and the neural network approach," *Journal of Electromagnetic Waves and Applications*, Vol. 7, No. 6, 873–893, 1993.
6. Ilavarason, P., J. E. Ross, E. J. Rothwell, K. M. Chen, and D. P. Nyquist, "Performance of an automated radar target discrimination scheme using E pulses and S pulses," *IEEE Trans. on Antennas and Propagation*, Vol. 42, No. 7, 582–588, 1993.
7. Rothwell, E. J., K. M. Chen, D. P. Nyquist, J. E. Ross, and R. Bebermeyer, "A radar target discrimination scheme using the discrete wavelet transform for reduced data storage," *IEEE Trans. on Antennas and Propagation*, Vol. 42, No. 7, 1033–1037, 1994.
8. Li, H. J., and Y. D. Wang, "Matching score properties between range profiles of high resolution radar targets," will appear in the *IEEE Trans. Antennas and Propagation*.
9. Mallet, S. G., "Multi-frequency channel decompositions of images and wavelet models," *IEEE Trans. Acoustic, Speech, and Signal Processing*, Vol. 37, No. 12, 2091–2110, 1989.
10. Mallat, S. G., "A theory for multi-resolution signal decomposition: the wavelet representation," *IEEE Trans. Pattern Analysis and Machine Intelligence*, Vol. 11, No. 7, 674–693, 1989.
11. Mallat, S. G., and S. Shong, "Characterization of signals from multiscale edges," *IEEE Trans. Pattern Analysis and Machine Intelligence*, Vol. 41, No. 7, 710–732, 1992.
12. Vetterli, M., and C. Horley, "Wavelet and filter bands: Theory and design," *IEEE Trans. Signal Processing*, Vol. 40, No. 9, 2207–2232, 1992.
13. Rioul, O., and M. Vetterli, "Wavelets and Signal Processing," *IEEE Signal Processing Magazine*, October 1991.
14. Li, H. J., and R. Y. Lane, "Utilization of multiple polarization data for aerospace target identification," will appear in the *IEEE Trans. Antennas and Propagations*.